Nanoscale Advances

ROYAL SOCIETY OF CHEMISTRY

PAPER

View Article Online
View Journal | View Issue

Cite this: *Nanoscale Adv.*, 2020, **2**, 3542

Bottom-up synthesis of titanophosphate nanosheets by the aqueous solution process†

Takayuki Ban, * Keito Asano, Chika Takai-Yamashita and Yutaka Ohya

The synthesis of titanophosphate nanosheets in aqueous sols was examined by the bottom-up process. The nanosheets were formed by mixing titanium iso-propoxide, phosphoric acid, and tetraalkylammonium hydroxide (NR_4OH) aqueous solutions, followed by diluting with water and heating at 80 °C, forming translucent aqueous sols of titanophosphate nanosheets with the same crystal structure as layered titanium phosphate $Ti_2O_3(H_2PO_4)_2 \cdot 2H_2O$. Whether the nanosheets were crystallized depended on the reactions during the mixing of reagents before the water dilution. By controlling the acid–base reactions between the Ti species, phosphoric acid, and the hydroxides of bulky cations in the aqueous sols, the one-pot process yielded highly water-dispersible, flake-like titanophosphate nanosheets. Under some synthetic conditions, nanosheets formed even in weakly basic aqueous sols. These nanosheets can be coated on a substrate with low alkali-resistance, or used for the removal of metal ions from neutral aqueous solutions.

Received 8th May 2020
Accepted 7th July 2020

DOI: 10.1039/d0na00376j

rsc.li/nanoscale-advances

Introduction

Metalate nanosheets are two-dimensional materials with highly anisotropic shapes; accordingly, they have attracted great interest. Electronic devices built from metalate nanosheets exhibit intriguing properties.[1–4] Aqueous sols of metalate nanosheets with large lateral size also possess interesting features, such as liquid crystallinity, optical trapping properties, and laser-induced mesostructual manipulation.[5–7] Conventionally, metalate nanosheets are synthesized by two-step ion exchanges, which intercalate bulky cations such as $N(C_4H_9)_4^+$ into the interlayers of layered metalates.[8–12] The intercalation of bulky cations leads to the exfoliation of layered metalates and the consequent formation of metalate nanosheets. Alternatively, we have formed metalate nanosheets by a bottom-up synthesis in aqueous solution.[12–18] The chemical reactions in the sols form layered metalates with bulky cations in their interlayers. These layered metalates are exfoliated, yielding metalate nanosheets as highly water-dispersible colloidal particles, which can be applied as coating sols for thin film fabrication by solution processes.[13,19] In our previous work, many types of metalate nanosheets were synthesized in strongly basic aqueous sols, which can corrode the substrates. To avoid this problem, bottom-up synthesis of metalate nanosheets in acidic or neutral aqueous sols is desirable. Because they flocculate, metalate nanosheets are also useful for the removal of metal ions from aqueous solutions. A further advantage of this application is the high dispersibility of nanosheets synthesized by the bottom-up process. However, metalate nanosheets synthesized by the bottom-up process are partially amorphous in neutral and acidic aqueous solutions.[20] Bottom-up synthesis in acidic or neutral aqueous solutions would expand the range of removal metal ions by the metalate nanosheets.

Titanate nanosheets ($Ti_{1.825}O_4^{0.7-}$) dispersed in transparent aqueous sols have been synthesized by mixing titanium iso-propoxide ($Ti[OCH(CH_3)_2]$; TIP) and tetramethylammonium hydroxide ($N(CH_3)_4OH$; TMAOH) aqueous solution in water by the bottom-up process.[12] The acid–base reactions between TMAOH and the TIP hydrolysis product $Ti(OH)_4$ yield layered titanates with interlayered cations TMA^+ in aqueous sols. The layered titanates are swollen and exfoliated, to form the titanate nanosheets. In such acid–base reactions, $Ti(OH)_4$ behaves as a very weak acid, so the aqueous solutions must be strongly basic. Instead, we envisaged the bottom-up synthesis of nanosheets using $Ti(OH)_4$ as a base. In this case, layered titanium phosphates would be formed by the acid–base reaction between phosphoric acid H_3PO_4 and $Ti(OH)_4$. Sequential acid–base reactions between the resulting layered titanium phosphates and TMAOH would lead to the exfoliation of the layered titanium phosphates, forming titanophosphate nanosheets. Mixing of TIP, H_3PO_4, and TMAOH can potentially yield titanophosphate nanosheets in neutral aqueous sols.

Department of Chemistry and Biomolecular Science, Gifu University, Yanagido 1-1, Gifu 501-1193, Japan. E-mail: ban@gifu-u.ac.jp; Tel: +81-58-293-2585

† Electronic supplementary information (ESI) available: XRD patterns of the layered titanium phosphates synthesized at different TIP/H_3PO_4 molar ratios, XRD patterns and Raman spectra of the thin films formed from titanophosphate nanosheet sols with different NR_4OH, XRD patterns of powders prepared from different titanophosphate nanosheet sols, TEM image of different titanophosphate nanosheets, and XRD pattern of the precipitates obtained by adding a mixture of amorphous phase and titanophosphate nanosheets to aqueous solution of copper acetate. See DOI: 10.1039/d0na00376j

Nanostructured titanium phosphates such as layered titanium phosphates can be used in various applications.[21–25] Among the known crystal structures of layered titanium phosphates are α-titanium phosphate ($Ti(HPO_4)_2\ H_2O$),[26] γ-titanium phosphate ($Ti(H_2PO_4)PO_4\ 2H_2O$),[26] π-titanium phosphate ($Ti_2O(PO_4)_2\ H_2O$),[27,28] and ρ-titanium phosphate ($Ti_2O(PO_4)_2\ H_2O$).[27,28] These layered titanium phosphates uptake alkaline and alkaline earth metal ions in aqueous solutions through ion-exchange reactions.[27] Yada *et al.* reported the presence of various micro- and nano-structures in layered titanium-phosphate thin films, which affect their wettabilities in water-drop test.[29] Moreover, nanocomposite thin films of silver nanoparticles and layered silver titanophosphates exhibit excellent antibacterial activities.[30] Different inorganic-organic nanocomposites of layered titanium phosphates and organic species have been extensively studied as metal species removers from aqueous solutions.[31–35] These layered titanium phosphates are hydrothermally synthesized by the bottom-up process in aqueous sols, but the bottom-up synthesis of titanophosphate nanosheets has not been reported. When forming titanophosphate nanosheets in aqueous sols, the acid–base reactions between Ti^{4+} species, phosphate ions, and bulky cations must be properly controlled.

This study has several objectives. We first synthesize titanophosphate nanosheets by the bottom-up process in aqueous sols, and then examine their formation mechanism. To this end, we study how the reactions between the Ti^{4+} species, phosphate ions, and bulky cations affect the titanophosphate nanosheet formation. Based on the obtained results, we also investigate the synthesis of titanophosphate nanosheets by the bottom-up process in neutral or very weakly basic aqueous sols. Finally, we investigate whether neutral or very weakly basic aqueous sols of titanophosphate nanosheets can form thin films on substrates with low alkali resistance, and/or remove metal ions from neutral aqueous solutions.

Experimental

Materials

TIP (1st grade), 85% phosphoric acid (guaranteed reagent), 2-propanol (1st grade), and copper acetate monohydrate (special grade) were purchased from FUJIFILM Wako Pure Chemical Co. Prior to use, TIP was distilled and 2-propanol was both dehydrated and distilled. The other reagents were used as received. The reagents of the tetraalkylammonium hydroxides are listed in Table 1.

Synthesis

Layered titanium phosphates were synthesized as follows: TIP (8.0 mmol) and 85% H_3PO_4 solution containing 8.0 mmol H_3PO_4 were mixed at room temperature for 2 h. The mixture was diluted by distilled water to 40 mL, and then stirred for 2 h. The Ti concentration in the reaction mixtures was 0.2 mol L^{-1}, and the molar ratio of TIP/H_3PO_4 was varied from 1/1 to 1/20. The aqueous mixtures were then transferred to a closed vessel, and heated at 60–150 °C for 1 day. The resultant precipitates containing layered titanium phosphate were collected by centrifugation, and then washed three times with 2-propanol.

Titanophosphate nanosheets were synthesized by the bottom-up process as follows: TIP (0.336 mmol), 85% H_3PO_4 solution (0.336 mmol of H_3PO_4), and tetraalkylammonium hydroxide (NR_4OH) aqueous solution were mixed at room temperature for 2 h. The used NR_4OH solutions are listed in Table 1. The mixture was diluted to 16.8 mL with distilled water. The Ti concentration in the resulting reaction sols was 0.2 mol L^{-1}, and the molar ratio of TIP/H_3PO_4 was 1/1. The reaction sols were transferred into a closed vessel, and heated at 80 °C for 1 day, forming titanophosphate nanosheet sols.

The influence of the mixing sequence of TIP, H_3PO_4, and TMAOH was investigated as follows: first, two out of the three reagents [TIP, 85% H_3PO_4 solution, and 25% TMAOH aqueous reagent (2.8 M)] were mixed at room temperature for 1 day. Next, the other reagent was added, and the mixture was stirred for 2 h. The molar ratio of the starting materials was TIP : H_3PO_4 : TMAOH = 1 : 1 : 2. The mixture was diluted to 0.2 mol-Ti L^{-1} with distilled water, and stirred at room temperature for 2 h. Finally, the resultant reaction sols were transferred to a closed vessel, and heated at 80 °C for 1 day.

The corrosion of glass substrates by titanophosphate nanosheet sols was investigated on Corning Eagle glass and borosilicate slide glass. The titanophosphate nanosheet sols (200 μL) were placed on the glass substrates (13 mm × 35 mm). The application was limited to 200 μL to avoid spillage of the sols

Table 1 NR_4OH reagents used

	Abbreviation	Concentration	
$N(CH_3)_4OH$	TMAOH	25% (2.8 M)	FUJIFILM Wako pure chemical (special grade)
		15% (1.6 M)	FUJIFILM Wako pure chemical (analytical grade)
		6% (0.7 M)	(Dilution of 15% TMAOH)
$N(C_2H_5)_4OH$	TEAOH	20% (1.4 M)	FUJIFILM Wako pure chemical (1st grade)
		10% (0.7 M)	FUJIFILM Wako pure chemical (special grade)
$N(C_3H_7)_4OH$	TPAOH	23% (1.1 M)	Tokyo chemical industry co. (The concentration was determined by titration)
		10% (0.5 M)	FUJIFILM Wako pure chemical (special grade)
$N(C_4H_9)_4OH$	TBAOH	40% (1.5 M)	Tokyo chemical industry co.
		20% (0.8 M)	(Dilution of 40% TMAOH)

from the substrate. The sols were evaporated on the substrates under ambient conditions.

The removal of aqueous Cu^{2+} by titanophosphate nanosheets was investigated as follows: copper acetate monohydrate ($Cu(OCOCH_3)_2\ H_2O$; 10 mmol) was dissolved in 20 mL of water. The titanophosphate nanosheet sols prepared at a TPAOH/TIP molar ratio of 2.2 were evaporated at approximately 4 kPa. After adding the resulting titanophosphate nanosheets (70 mg) to the copper acetate aqueous solution, the mixture was stirred for 3 days at room temperature. The precipitates and supernatant were then separated by centrifugation, and the precipitates were washed in mixed 2-propanol and water for 3 min by centrifugation at 6000 rpm.

Characterization

X-ray diffraction (XRD) measurements were performed on a Rigaku Ultima IV diffractometer with monochromatic CuKα irradiation. The XRD patterns were recorded at 2° min^{-1} in the 2θ range 2° to 70°.

Transmission electron microscopy (TEM) images were captured by a JEOL JEM-2100 system at an accelerating voltage of 200 kV. The samples were prepared by evaporating a drop of sample sol onto a Cu grid supported with a Formvar thin film. The Cu grid was subjected to hydrophilic treatment before use.

The Raman spectra were acquired on a JASCO NRS-1000 model using a 532 nm incident beam in the Raman shift range 200–1500 cm^{-1}. The exposure period was 5–20 s. The number of accumulations was set to 3.

Atomic force microscope (AFM) images were captured on a Seiko instrument SPI3800 model by using a silicon tip cantilever (16 N m^{-1}) in tapping mode. The samples were prepared by dropping diluted nanosheet sols on a mica substrate, followed by drying at 100 °C for 10 min.

Ultraviolet-visible (UV-vis) spectra were measured on a Hitachi U-4100 model using a dual beam in transmittance mode. The samples in solution were transferred into the quartz glass cuvette (10 × 10 × 45 mm^3), and their spectra were recorded from 1000 nm to 200 nm at 300 nm min^{-1}.

The pH values of the aqueous sols were measured by a Horiba D-54 model. The electrode for measurements of strongly basic solutions (Horiba 9632-10D model) was used.

Results and discussion

Bottom-up synthesis of layered titanium phosphate in aqueous solution

Titanophosphate nanosheets are prepared by exfoliating layered titanium phosphates. Some of the known types of layered titanium phosphates were described in the Introduction section. We first examined the crystal structure of layered titanium phosphate synthesized by the bottom-up process. TIP and H_3PO_4 were mixed at a molar ratio of 1 : 1, yielding an amorphous mixture. After heating at 60–150 °C, layered titanate with a chemical composition of $Ti_2O_3(H_2PO_4)_2\cdot 2H_2O$[31] was obtained (Fig. 1). The $Ti_2O_3(H_2PO_4)_2\cdot 2H_2O$ crystallized at low pH (~2). When H_3PO_4 was added in large amounts (*i.e.*, at H_3PO_4/TIP ≥ 5) and the mixture was heated at 100 °C, α-layered titanium phosphate was formed (Fig. S1 in the ESI†). However, under the synthetic conditions of the present study, other layered titanium phosphates were not formed.

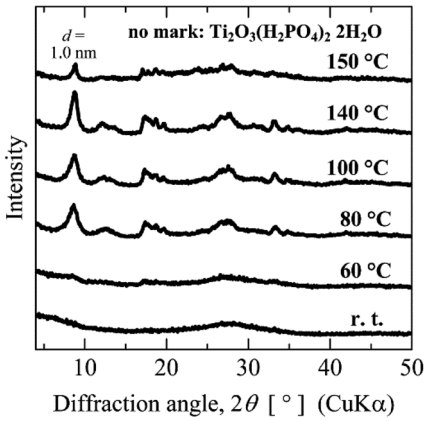

Fig. 1 XRD patterns of layered titanium phosphates synthesized by heating the aqueous mixture of TIP and H_3PO_4 at different temperatures.

Fig. 2b shows the morphology (TEM image) of the layered titanium phosphate $Ti_2O_3(H_2PO_4)_2\cdot 2H_2O$ synthesized at 80 °C. The titanium phosphate nanosheets were precipitated as agglomerated particles approximately 1 μm in size (Fig. 2a). Thus, the titanium phosphate nanosheets were probably agglomerated in the aqueous sols, but not exfoliated.

Bottom-up synthesis of titanophosphate nanosheets in aqueous sols

The bottom-up synthesis of titanophosphate nanosheets was examined by reacting TIP, H_3PO_4, and NR_4OH in aqueous sols.

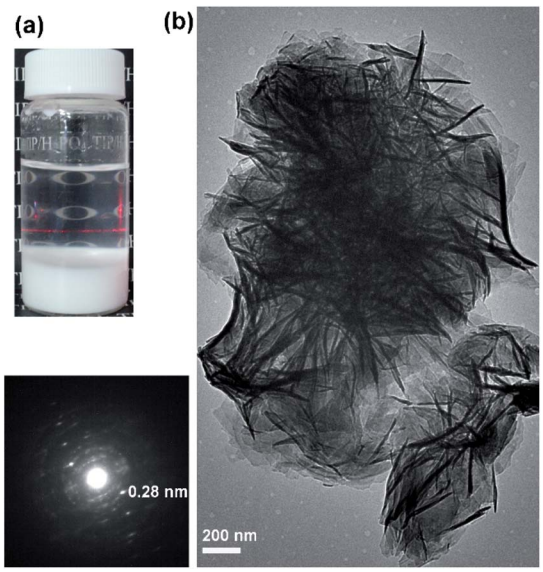

Fig. 2 (a) Appearance, (b) TEM images, and electron diffraction pattern of layered titanium phosphates synthesized by heating the aqueous mixture of TIP and H_3PO_4 at 80 °C.

As mentioned above, a 1 : 1 molar ratio of TIP and H_3PO_4 reacted to form a layered titanium phosphate $Ti_2O_3(H_2PO_4)_2 \cdot 2H_2O$. The added NR_4OH is expected to react with $Ti_2O_3(H_2PO_4)_2 \cdot 2H_2O$ by an acid–base reaction, intercalating the bulky cations NR_4^+ into the interlayers of the layered titanium phosphate, and eventually forming titanophosphate nanosheets by the swelling and exfoliation of layered titanium phosphate. In this experiment, TIP, 85% H_3PO_4 solution, and 25% TMAOH solution were mixed at a molar ratio of 1/1/2 and then diluted by water. The pH of the sol was approximately 8. After heating the mixtures at 80 °C, translucent aqueous sols were yielded (Fig. 3a), which were evaporated on a glass substrate. In the XRD patterns of the obtained thin films, the *d*-spacings between the peaks were ordered as 1 : 1/2 : 1/3, indicating a highly oriented layered compound (Fig. 3b). That is, titanophosphate nanosheets were formed by the bottom-up process in aqueous sols. After synthesis, the nanosheet sols remained intact even after several months of storage. Moreover, the basal spacing of the layered compounds (~1.7 nm, obtained in stacked titanophosphate nanosheets) was independent of the type of alkylammonium ions except in the synthesis using TBAOH (see Fig. S2 in the ESI†). The spacing was larger in the layered compounds than in $Ti_2O_3(H_2PO_4)_2 \cdot 2H_2O$ (1.0 nm). The basal spacing was probably largely influenced by the water molecules in the interlayer. Meanwhile, the Raman spectra of the titanophosphate nanosheets and layered titanium phosphate were similar, but with shifted peaks (Fig. 3c). The removal of H^+ from the $Ti_2O_3(H_2PO_4)_2$ layers and the exfoliation process likely distorted the titanophosphate layers. The Raman spectra of the titanophosphate nanosheets prepared from TEAOH and TPAOH were also measured (Fig. S3 in the ESI†). The Raman spectra were independent of the NR_4OH type used in the synthesis, indicating that the titanophosphate nanosheets prepared from TEAOH and TPAOH had the same structure as those prepared from TMAOH.

The morphology of the titanophosphate nanosheets was investigated by TEM. The titanophosphate nanosheets were flake-like shapes (Fig. 4a) with much smaller lateral sizes (5 to 50 nm) than layered titanium phosphate $Ti_2O_3(H_2PO_4)_2 \cdot 2H_2O$. Moreover, in high-resolution TEM images, lattice fringes with an interval of ~0.28 nm were observed (Fig. 4b). This interval was very close to the *d*-spacing of diffraction spot in the electron diffraction of $Ti_2O_3(H_2PO_4)_2 \cdot 2H_2O$ (see Fig. 2). These results confirmed the similar crystal structure of titanophosphate nanosheets and $Ti_2O_3(H_2PO_4)_2 \cdot 2H_2O$. Furthermore, the AFM images of the titanophosphate nanosheets revealed many flake-

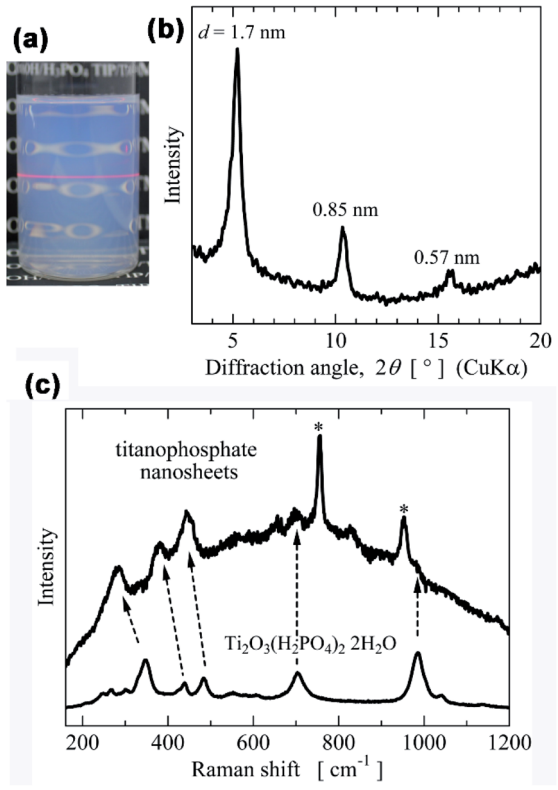

Fig. 3 (a) Appearance, (b) XRD pattern and (c) Raman spectra of titanophosphate nanosheets synthesized by heating of the aqueous mixture of TIP, H_3PO_4, and TMAOH with a molar ratio of TIP : H_3PO_4 : TMAOH = 1 : 1 : 2 at 80 °C. The marks * are assigned to TMA^+ ion.

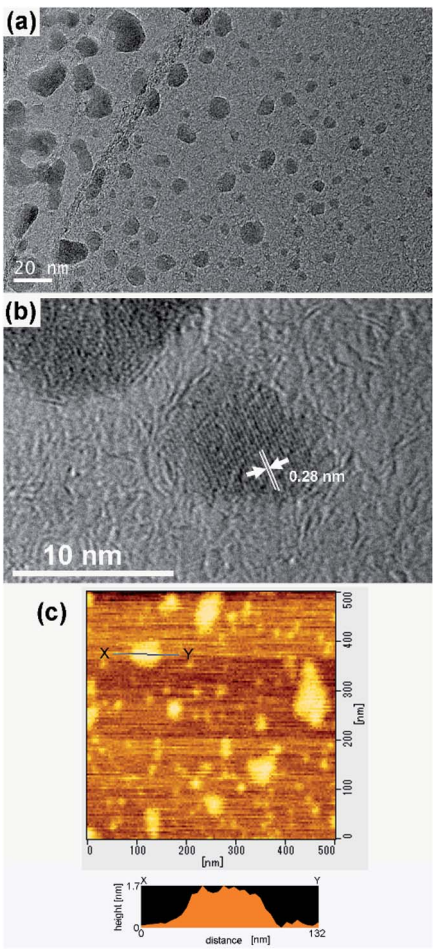

Fig. 4 (a and b) TEM and (c) AFM images of titanophosphate nanosheets synthesized by heating of the aqueous mixture of TIP, H_3PO_4, and TMAOH with a molar ratio of TIP : H_3PO_4 : TMAOH = 1 : 1 : 2 at 80 °C.

like nanosheets of monolayer thickness (~1.5 nm, Fig. 4c). We surmised that many of the titanophosphate nanosheets existed as monolayers in the aqueous sols.

Influence of mixing sequence of the reagents on the formation of titanophosphate nanosheets

Titanophosphate nanosheets were synthesized by acid–base reactions between H_3PO_4 and $Ti(OH)_4$, followed by acid–base reactions between the obtained $Ti_2O_3(H_2PO_4)_2 \cdot 2H_2O$ and NR_4OH. Thus, the addition sequence of TIP, H_3PO_4 and NR_4OH should influence the formation of titanophosphate nanosheets. To explore this influence, two of three reagents [TIP, H_3PO_4 (85%), and TMAOH (25%)] were mixed for 1 day. Next, the other reagent was added, and the mixture was stirred for 2 h, then diluted with water. The pH of the sols prepared by all mixing sequence was approximately 8. Finally, the mixture was heated at 80 °C for 1 day. Fig. 5 shows the experimental results of mixing TIP : H_3PO_4 : TMAOH at a molar ratio of 1 : 1 : 2 and heating at 80 °C.

Although adding the reagents in any sequence yielded titanophosphate nanosheets, the amount of the formed nanosheets depended on the addition sequence, and increased in the following order: (H_3PO_4 + TMAOH) + TIP < (TIP + H_3PO_4 + TMAOH) < (TIP + TMAOH) + H_3PO_4 < (TIP + H_3PO_4) + TMAOH. The nanosheet yield was maximized by initially mixing TIP and H_3PO_4 and later adding TMAOH. This indicates that the proposed reactions – formation of layered titanium phosphate by the acid–base reaction of TIP and H_3PO_4, followed by the acid–base reaction of layered titanium phosphate and TMAOH – achieved the bottom-up synthesis of titanophosphate nanosheets.

The initial mixing of TIP and TMAOH followed by H_3PO_4 addition also obtained a high nanosheet yield. The TIP and TMAOH formed titanate nanosheet sols. When H_3PO_4 was added, it favourably reacted with the titanate nanosheets to form titanophosphate nanosheets.

The initial mixing of H_3PO_4 and TMAOH followed by TIP addition provided the smallest nanosheet yield. The neutral solution formed by mixing H_3PO_4 and TMAOH probably reduced the reactivity of the Ti species formed by TIP hydrolysis. Thus, the reaction of the Ti species with H_3PO_4 or NR_4OH played an important role in the bottom-up synthesis of the titanophosphate nanosheets.

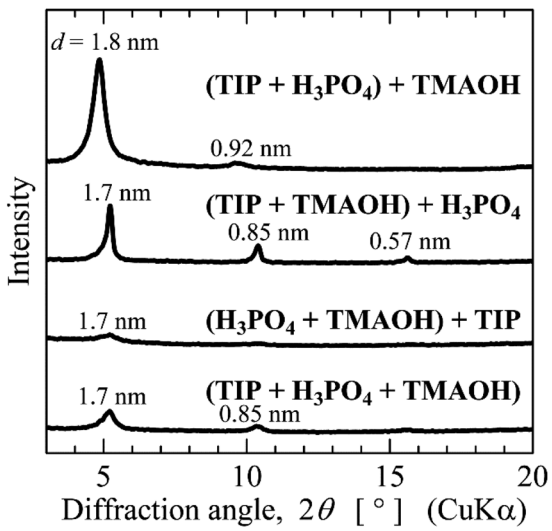

Fig. 5 XRD patterns of the thin films fabricated by evaporating the titanophosphate nanosheet sols prepared by different mixing sequences of TIP, 85% H_3PO_4 solution, and 25% TMAOH solution at a molar ratio of TIP : H_3PO_4 : TMAOH = 1 : 1 : 2.

One-pot synthesis of titanophosphate nanosheets by using different NR_4OH reagents

NR_4OH aqueous solution reagents with different concentrations are commercially available. To test whether the concentrations of NR_4OH reagents influence the nanosheet formation, the NR_4OH concentrations and types were varied in the one-pot synthesis of titanophosphate nanosheet sols. The NR_4OH solutions (TMAOH, TEAOH, TPAOH, and TBAOH) were added at low (0.5–0.8 M) and high (1.1–1.6 M) concentrations, and the obtained products were compared. First, the TIP, 85% H_3PO_4 aqueous solution and NR_4OH solutions were mixed for 2 h, and the mixtures were diluted with water. For all samples, the Ti and P concentrations were adjusted to 0.2 M by the H_2O addition. The pH values of the sols depended on the NR_4OH/Ti^{4+} ratios as shown in Table 2, but were independent of the types and concentrations of the NR_4OH solutions. To crystallize the titanophosphate nanosheets, the aqueous mixtures were heated at 80 °C for 1 day. Fig. 6 compares the XRD patterns of the thin films fabricated from the TIP : H_3PO_4 : TPAOH = 1 : 1 : 2.2 sols prepared at low and high concentrations of TPAOH. When added at low concentrations, the TPAOH solutions obtained very high yields of titanophosphate nanosheets, but the high-concentration TPAOH solutions obtained very few nanosheets. Obviously, the concentration of the TPAOH reagent influenced the titanophosphate nanosheet formation. Thus, the crystallization of titanophosphate nanosheets was determined by the reactions during the mixing before dilution by water.

Table 2 Influence of the concentration of NR_4OH solutions on the crystallization of titanophosphate nanosheets[a]

	1TIP : 1H_3PO_4 : xNR_4OH			
x=	2.0 (pH 8)	2.2 (pH 9)	2.3 (pH 10)	2.5 (pH 11)
High concentration				
TMAOH (1.6 M)	×	×	×	O
TEAOH (1.4 M)	Δ	×	×	×
TPAOH (1.1 M)	×	×	×	×
TBAOH (1.5 M)	×	×	×	×
Low concentration				
TMAOH (0.7 M)	×	×	Δ	Δ
TEAOH (0.7 M)	×	Δ	Δ	O
TPAOH (0.5 M)	Δ	OO	OO	O
TBAOH (0.8 M)	×	×	×	×

[a] The marks OO, O, Δ, and × represent that the amounts of formed titanophosphate nanosheets were very large, large, medium, and small, respectively.

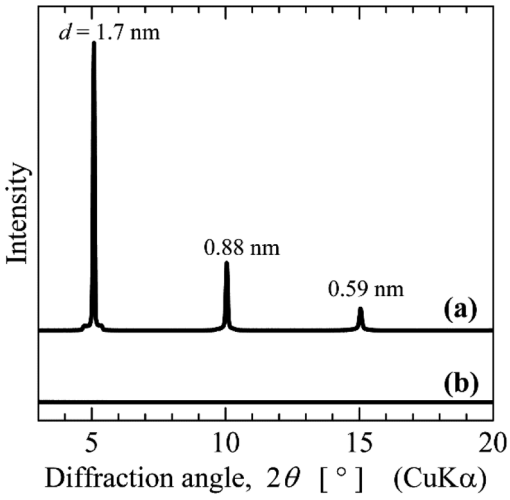

Fig. 6 XRD patterns of the thin films fabricated by evaporating the titanophosphate nanosheet sols prepared by using TPAOH solutions with (a) low and (b) high concentrations (0.5 and 1.1 M) at a molar ratio of TIP : H_3PO_4 : TPAOH = 1 : 1 : 2.2.

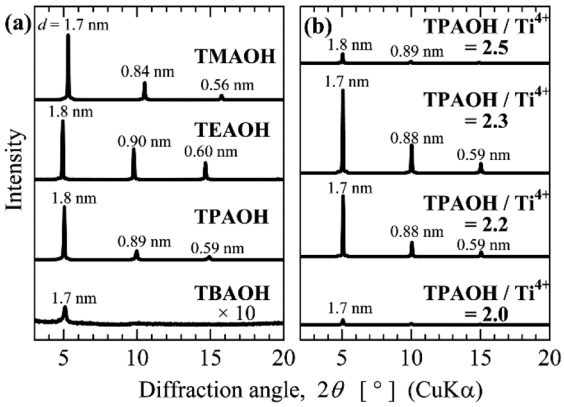

Fig. 7 XRD patterns of the thin films fabricated by evaporating (a) the titanophosphate nanosheet sols prepared by using different NR_4OH solutions at a molar ratio of TIP : H_3PO_4 : NR_4OH = 1 : 1 : 2.5, and (b) the nanosheet sols prepared by using 0.5 M TPAOH solutions at different TPAOH/TIP molar ratios of 2.0 to 2.5.

Table 2 lists the titanophosphate nanosheet syntheses in various NR_4OH solutions at different molar ratios of NR_4OH/Ti^{4+}. The amounts of synthesized titanophosphate nanosheets were evaluated from the peak intensities in the XRD patterns of the thin films formed from the nanosheet sols. The XRD measurements of some samples were performed on powders prepared by evaporating the nanosheet sols (Fig. S4 in the ESI†). The high correlation of XRD peak intensities between powder and thin film samples confirmed that the amount of titanophosphate nanosheets can be determined from the XRD patterns of the thin films fabricated from nanosheet sols.

In general, the diluted NR_4OH solutions yielded more titanophosphate nanosheets than highly concentrated solutions, but there were some exceptions, such as TMAOH/Ti^{4+} = 2.5. As mentioned above, the initial mixing of NR_4OH with H_3PO_4 produced few titanophosphate nanosheets, whereas reacting Ti species with NR_4OH or H_3PO_4 facilitated the nanosheet formation. These results imply that highly concentrated NR_4OH solutions facilitated the reactions of NR_4OH with H_3PO_4, whereas lowly concentrated NR_4OH solutions facilitated the reactions of Ti species with NR_4OH or H_3PO_4. Moreover, increasing the length of the alkyl chain in NR_4^+ enhanced the effect of NR_4OH concentration on the titanophosphate nanosheet formation, and extended the region of nanosheet formation toward neutral conditions (except in the TBAOH cases). The alkyl chain length and hydration of NR_4^+ probably largely influenced the titanophosphate nanosheet formation. Therefore, we infer that hydration of an appropriate NR_4^+ type will facilitate the reactions of NR_4OH with Ti species.

Fig. 7a shows the XRD patterns of the layered titanophosphate thin films fabricated by evaporating the titanophosphate nanosheet sols prepared from highly concentrated TMAOH and TBAOH and lowly concentrated TEAOH and TPAOH (NR_4OH/Ti^{4+} = 2.5). The XRD pattern of the sample prepared from lowly concentrated TPAOH (TPAOH/Ti^{4+} = 2.0–2.5) is shown in Fig. 7b. Fig. 7 shows the results of the samples yielding the largest amounts of titanophosphate nanosheets for each NR_4OH. At a NR_4OH/Ti^{4+} ratio of 2.5, the yields of titanophosphate nanosheets were similar in TMAOH, TEAOH, and TPAOH, but TBAOH yielded few nanosheets. Likely, the TBA^+ ion was too large and bulky to intercalate in the layered titanophosphate. In contrast, the TPAOH preparation obtained a large amount of titanophosphate nanosheets even in very weakly basic sols (pH $\sim$ 9 for TPAOH/Ti^{4+} = 2.2). TEM images of the formed nanosheets are shown in Fig. S5a in the ESI.† Flake-like nanosheets were observed. TEM images of the titanophosphate nanosheets synthesized from other sols are given in Fig. S5 in the ESI.† The lateral size of the synthesized titanophosphate nanosheets ranged from approximately 5 nm to 20 nm, and the structures were flake-like. As mentioned above, the 25% TMAOH reagent (2.8 M) at a TMAOH/Ti^{4+} ratio of 2.0 also obtained a relatively high nanosheet yield at pH 8, when the adding sequence was (TIP + H_3PO_4) + TMAOH. Thus, under the appropriate synthetic conditions, titanophosphate nanosheets were formed even in very weakly basic aqueous sols.

Influence of the basicity of titanophosphate nanosheet sols on the corrosion of substrates

Borosilicate glass may corrode in basic aqueous solutions, because silicate or borate reacts with OH^- ion. The corrosion of glass substrates might contaminate thin film with alkaline ions released from the glass, thereby degrading its quality. As the titanophosphate nanosheet sols were synthesized in very weakly basic aqueous sols by the bottom-up process, glass substrates should not be corroded by the sols. Therefore, the aqueous sols in this study are suitable for thin-film fabrication by the sol–gel method or the chemical bath deposition method. To verify that the corrosion of glass substrates was inhibited by our method, we tested two glass substrates: Corning Eagle glass and a borosilicate slide glass with high and low resistance to alkalis, respectively. The titanophosphate nanosheet sols prepared at

TPAOH/Ti^{4+} ratios of 2.2 (pH 9) and 2.5 (pH 11) were placed on the glass substrates, and evaporated under ambient conditions. The XRDs of the resulting thin films are shown in Fig. 8. The thin film formed from nanosheet sols with pH ~11 exhibited very sharp diffraction peaks of layered titanophosphate (resulting from the stacked titanophosphate nanosheets) on Eagle glass, but weak, broad, and split peaks on the borosilicate glass substrate. The peak degradation was likely attributable to corrosion of the substrate and consequent contamination by alkaline species. Conversely, the films formed from the nanosheet sols with pH ~ 9 exhibited very sharp XRD peaks on both the Eagle glass and borosilicate glass substrates. Thus, titanophosphate nanosheet sols prepared by the bottom-up process in aqueous solution yielded layered titanophosphate thin films even on low-alkali resistant glass.

Removal of Cu^{2+} ion from neutral aqueous solutions by the titanophosphate nanosheets

Owing to their flocculation and ion-exchange behaviours, metalate nanosheets and layered metalates are effective removers of metal ions from aqueous solutions. To examine the removal of metal ions from neutral aqueous solution, we employed the titanophosphate nanosheets obtained in very weakly basic aqueous sols. The titanophosphate nanosheet sols prepared at TPAOH/Ti^{4+} = 2.2 (pH 9) were evaporated to form a layered titanophosphate powder. When this powder was added to aqueous solutions of copper acetate (Cu^{2+} = 0.01 mol L^{-1}), precipitates were formed and the colour of the $Cu(OCOCH_3)_2$ aqueous solution changed from bluish to colourless (Fig. 9a). After adding the nanosheet powder, the absorption around 800 nm vanished from the UV-vis spectrum (Fig. 9a). The XRD measurements showed that the precipitates were amorphous (Fig. 9b). When a mixture of amorphous phase and titanophosphate nanosheets was added to $Cu(OCOCH_3)_2$ aqueous solution, the formed precipitates included anatase-type TiO_2 (Fig. S6 in the ESI†). As the titanophosphate nanosheets prepared at TPAOH/Ti^{4+} = 2.2 (pH 9) did not form anatase precipitates, the amorphization of titanophosphate nanosheets did not occur, and Cu^{2+} was probably removed by the flocculation of titanophosphate nanosheets.

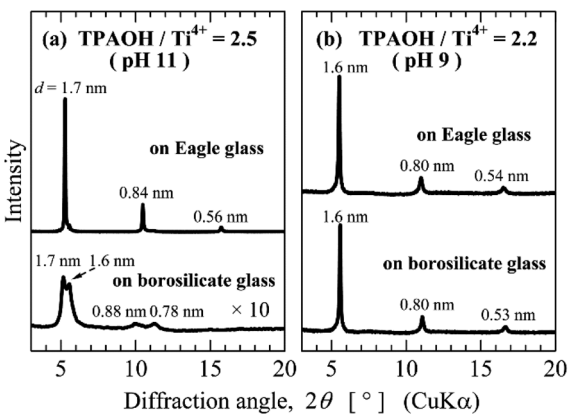

Fig. 8 XRD patterns of the thin films fabricated by evaporating the titanophosphate nanosheet sols, which were prepared at a molar ratio of TIP : H_3PO_4 : TPAOH = 1 : 1 : (a) 2.5 and (b) 2.2, on Eagle glass and borosilicate glass substrates.

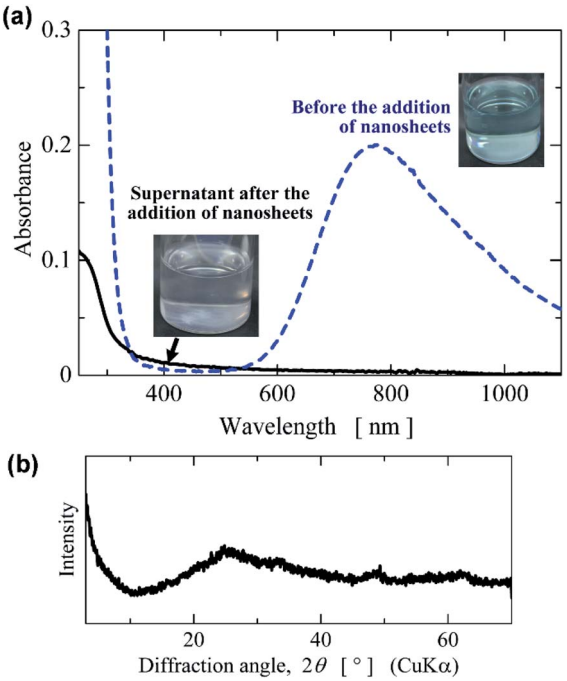

Fig. 9 (a) Appearance and UV-vis spectra of copper acetate aqueous solutions before and after the addition of titanophosphate nanosheets. (b) XRD pattern of the precipitates obtained by adding titanophosphate nanosheets to copper acetate aqueous solution.

Conclusions

Previously, we synthesized metalate nanosheets by a bottom-up aqueous solution process. However, in many cases, the nanosheet synthesis required strongly basic aqueous sols. In thin film fabrication by solution processes, strongly basic solutions are undesirable because they corrode the substrates. In this study, highly water-dispersible titanophosphate nanosheets were synthesized by the bottom-up process in very weakly basic aqueous sols. With controlled acid–base reactions among the NR_4OH, Ti^{4+} species and H_3PO_4 in the one-pot synthesis, an aqueous mixtures of TIP, H_3PO_4, and NR_4OH yielded titanophosphate nanosheets at high yield. Specifically, the alkyl chain length and hydration state of NR_4^+ influenced the reaction between NR_4OH and the Ti species. Moreover, the resulting titanophosphate nanosheets had the same crystal structure as layered titanium phosphate $Ti_2O_3(H_2PO_4)_2 \cdot 2H_2O$. The nanosheets were flake-like with a lateral size of 5–50 nm. Furthermore, as the titanophosphate nanosheets were synthesized in very weakly basic sols, the resulting aqueous sols can be coated as nanosheets on glass substrates with low alkali resistance. In flocculated form, the nanosheets can also sequester Cu^{2+} ions from neutral aqueous solutions.

The results of this study will guide the synthesis of other metallophosphate nanosheets, and can expand the applications of nanosheets synthesized by bottom-up processes.

Conflicts of interest

There are no conflicts to declare.

Acknowledgements

This study was supported by KAKENHI (Grant-in-Aid for Scientific Research 17K06014) from Japan Society for the Promotion of Science (JSPS).

Notes and references

1 M. Osada and T. Sasaki, *J. Mater. Chem.*, 2009, **19**, 2503–2511.
2 J. L. Gunjakar, I. Y. Kim, J. M. Lee, Y. K. Jo and S.-J. Hwang, *J. Phys. Chem. C*, 2014, **118**, 3847–3863.
3 M. Osada, Y. Ebina, H. Funakubo, S. Yokoyama, T. Kiguchi, K. Takada and T. Sasaki, *Adv. Mater.*, 2006, **18**, 1023–1027.
4 S. Sekizaki, M. Osada and K. Nagashio, *Nanoscale*, 2017, **9**, 6471–6477.
5 T. Nakato and N. Miyamoto, *Materials*, 2009, **2**, 1734–1761.
6 N. Miyamoto and T. Nakato, *Isr. J. Chem.*, 2012, **52**, 881–894.
7 T. Nakato, Y. Higashi, W. Ishitobi, T. Nagashita, M. Tominaga, Y. Suzuki, T. Iwai and J. Kawamata, *Langmuir*, 2019, **35**, 5568–5573.
8 T. Sasaki, M. Watanabe, H. Hashizume, H. Yamada and H. Nakagawa, *J. Am. Chem. Soc.*, 1996, **118**, 8329–8335.
9 T. Sasaki, M. Watanabe, H. Hashizume, H. Yamada and H. Nakagawa, *Chem. Commun.*, 1996, 229–230.
10 M. Osada and T. Sasaki, *Adv. Mater.*, 2012, **24**, 210–228.
11 R. Ma and T. Sasaki, *Adv. Mater.*, 2010, **22**, 5082–5104.
12 T. Ohya, A. Nakayama, T. Ban, Y. Ohya and Y. Takahashi, *Chem. Mater.*, 2002, **14**, 3082–3089.
13 T. Ban, S. Yoshikawa and Y. Ohya, *J. Colloid Interface Sci.*, 2011, **364**, 85–91.
14 T. Ban, S. Yoshikawa and Y. Ohya, *CrystEngComm*, 2012, **14**, 7709–7714.
15 T. Ban, T. Ito and Y. Ohya, *Inorg. Chem.*, 2013, **52**, 10520–10524.
16 T. Ban, S. Iriyama and Y. Ohya, *Adv. Powder Technol.*, 2018, **29**, 537–542.
17 T. Ban, T. Wakita, R. Yokoyama, T. Miyake and Y. Ohya, *CrystEngComm*, 2018, **20**, 3559–3568.
18 T. Ban, T. Kaiden and Y. Ohya, *Cryst. Growth Des.*, 2019, **19**, 6903–6910.
19 T. Ban, T. Ito and Y. Ohya, *J. Sol-Gel Sci. Technol.*, 2013, **68**, 88–94.
20 T. Ban, T. Nakagawa and Y. Ohya, *Cryst. Growth Des.*, 2015, **15**, 1801–1807.
21 H. Li, Y. Sun, Z.-Y. Yuan, Y.-P. Zhu and T.-Y. Ma, *Angew. Chem., Int. Ed.*, 2018, **57**, 3222–3227.
22 Y. Zhu, G. Hasegawa, K. Kanamori and K. Nakanishi, *Inorg. Chem. Front.*, 2018, **5**, 1397–1404.
23 A. Bhaumik and S. Inagaki, *J. Am. Chem. Soc.*, 2001, **123**, 691–696.
24 Z. Yin, Y. Sakamoto, J. Yu, S. Sun, O. Terasaki and R. Xu, *J. Am. Chem. Soc.*, 2004, **126**, 8882–8883.
25 J. Peng, L.-N. Feng, Z.-J. Ren, L.-P. Jiang and J.-J. Zhu, *Small*, 2011, **7**, 2921–2928.
26 A. N. Christensen, E. K. Anderson, I. G. Anderson, G. Albrti, M. Nielsen and M. S. Lehmann, *Acta Chem. Scand.*, 1990, **44**, 865–872.
27 A. I. Bortun, S. A. Khainakov, L. N. Bortun, D. M. Poojary, J. Rodriguez, J. R. Garcia and A. Clearfield, *Chem. Mater.*, 1997, **9**, 1805–1811.
28 D. M. Poojary, A. I. Bortun, L. N. Bortun and A. Clearfield, *J. Solid State Chem.*, 1997, **132**, 213–223.
29 M. Yada, Y. Inoue, A. Sakamoto, T. Torikai and T. Watari, *ACS Appl. Mater. Interfaces*, 2014, **6**, 7695–7704.
30 M. Yada, Y. Inoue, T. Morita, S. Imamura, T. Torikai and T. Watari, *Thin Solid Films*, 2017, **628**, 184–189.
31 L. Kőrösi, S. Papp and I. Dékány, *Chem. Mater.*, 2010, **22**, 4356–4363.
32 W. Zhang, S. Hietala, L. Khriachtchev, T. Hatanpää, B. Doshi and R. Koivula, *ACS Appl. Mater. Interfaces*, 2018, **10**, 22083–22093.
33 C. Chen, Y.-L. Yang, K.-L. Huang, Z.-H. Sun, W. Wang, Z. Yi, Y.-L. Liu and W.-Q. Pang, *Polyhedron*, 2004, **23**, 3033–3042.
34 O. A. Khainakova, A. Espina, C. Trobajo, S. A. Khainakov, J. R. Garcia and A. I. Bortan, *Stud. Surf. Sci. Catal.*, 2002, **144**, 701–708.
35 A. Hayashi, H. Nakayama and M. Tsuhako, *Bull. Chem. Soc. Jpn.*, 2002, **75**, 1991–1996.